Phys. Status Solidi A **211,** No. 1, 126–130 (2014) / **DOI** 10.1002/pssa.201300127

physica status solidi a
www.pss-a.com
applications and materials science

# Atom-probe tomography study of boron precipitation in highly implanted silicon

**Didier Blavette*, Huiyuan Wang, Manon Bonvalet, Florian Hüe, and Sébastien Duguay**

Normandie University, GPM, UMR CNRS 6634, BP 12, 76801 St Etienne du Rouvray cedex, France

Received 16 May 2013, revised 9 October 2013, accepted 31 October 2013
Published online 5 December 2013

**Keywords** atom probe tomography, boron, precipitation, silicon

* Corresponding author: e-mail didier.blavette@univ-rouen.fr, Phone: +33 232955035, Fax: +33 232955032

Precipitation of boron in heavily doped silicon has been investigated using transmission electron microscopy (TEM) and atom-probe tomography (APT). Si wafers were implanted with a very high boron dose ($1 \times 10^{17}$ at. $cm^{-2}$) at 27 keV and further annealed at 500, 750 and 1000 °C for 1 h. Results show that precipitates nucleate during implantation before any annealing has been made. They were found to have a smaller boron content than that of the expected phase $SiB_3$. With increasing thermal budget, the concentration of boron approaches the equilibrium composition 75 at.%. It is thought that small boron-enriched precipitated clusters that form in supersaturated silicon should be distinguished from the boron interstitial clusters (BICs).



**1 Introduction** The dopant distribution in implanted silicon is of crucial importance for recent CMOS transistors (complementary metal oxide semiconductor). Indeed, the miniaturization of CMOS devices is accompanied by electrical characteristic dispersion that can have dramatic effects on a technology node. Such dispersion might be the result of dopant redistribution to defects in the semiconductor or due to its precipitation when exceeding the solubility limit in the semiconductor. As far as p-type doping in silicon is concerned, boron has been extensively studied by the semiconductor industry over the last decades. Usually introduced in Si by ion implantation to create controlled dopant profiles, boron can, however, interact with the defects generated during the implantation step. Boron atoms are nowadays usually implanted at concentrations exceeding their solid solubility limit, thus leading to precipitation.

Laser-assisted atom-probe tomography (APT) is a unique approach to observe and characterize boron precipitation in 3D at the nm scale [1, 2]. As an example, APT showed that n-type dopants such as As and P decorated end-of-range defects in implanted Si or polycrystalline Si [3]. The distribution of implanted boron was also recently studied using APT. At concentrations above its solubility limits and after annealing, B–Si nanoprecipitates were observed [4]. The latter were then assimilated to metastable precipitates of B and clearly linked to be responsible for the electrical deactivation of B in Si. These boron-enriched precipitates were sometimes identified as boron interstitial clusters (BICs) although they contain a large number of atoms and their formation is driven by the boron supersaturation. This issue will be discussed later in the present paper. To understand boron precipitation in implanted Si more deeply, but also to assess the quantitative limits of APT, highly supersaturated samples were investigated.

**2 Experimental** [100]-oriented p-type Si wafers, originally doped at $\sim 10^{19}/cm^3$ with boron were first prepared using the reactive ion etching Bosch process, transforming them into flat-topped silicon posts (6 μm in diameter and 100 μm in height, the post spacing was close to 50 μm). Pieces of the wafer were then implanted with a very high dose ($10^{17}$ at. $cm^{-2}$) of boron. It should be noted that such a high dose is not common in microelectronics. The energy of implantation was chosen as 27 keV in order to get a maximum concentration located at around 100 nm below the surface. Pieces of the sample were annealed at 500, 750 and 1000 °C under $N_2$ for 1 h in order to form boride precipitates. The nonannealed sample is referred to as NA.

APT analyses require samples to be prepared in the shape of sharply pointed needles. For that purpose, silicon

posts were nanomilled in the form of 50-nm end radius tips using a focused ion beam (FIB) system. An *in situ* deposited Pt cap was used to limit gallium implantation during ion milling ($Ga^+$, 30 keV) of both the surface and the doped area. A final cleaning of the tip with a 2-keV gallium beam was then performed in order to eliminate the Pt cap and implantation damages. The FIB equipment used to prepare APT samples was a ZEISS NVISION 40.

APT characterizations were performed using a CAMECA LAWATAP instrument. An amplified ytterbium-doped laser operating at a wavelength of 343 nm, with 350-fs pulse duration and a 100-kHz repetition rate was used. During the analysis, the tip was cooled at a temperature of 80 K and the energy per pulse was chosen in order to obtain a constant $Si^{2+}/Si^+$ count ratio for analysis reproducibility. More details on laser-assisted APT can be found elsewhere [5].

Secondary ion mass spectrometry (SIMS) analyses (Fig. 1) were also conducted and concentration profiles were obtained using an isotopic comparative method especially developed for high boron concentration in Si [6]. Note that APT data were calibrated in depth using the SIMS data.

Complementary transmission electron microscopy (TEM) investigations of 1000 °C samples were conducted using a JEOL ARM200 HRTEM. Silicon posts were mounted to a TEM grid and then thinned by FIB. A 2-keV final step was also used to limit the damaged region due to the Ga ion beam. TEM lamella thickness was measured to be 60 nm by electron energy loss spectroscopy (EELS). Scanning transmission electron microscopy (STEM) and EELS analysis were used to validate the implantation depth and the maximum concentration.

In contrast to SIMS, APT measurements of compositions are in principle quantitative since all elements evaporated from the tip surface have the same probability to be ionized (100%) and are detected with the same efficiency (~50%). However, because of its high evaporation field (64 V/nm versus 33 V/nm for silicon), boron atoms are prone to drastic retention effects, hence leading to evaporation bursts. This is particularly observed in B-enriched regions in silicon (clusters, interfacial segregation, etc.). These bursts push detectors beyond their utmost limits. Two simultaneous ion impacts on the detector may then be taken as a single impact, biasing thus both the position of impacts and composition data (two boron atoms or more may be interpreted as a single atom). This problem leads to underestimated boron contents, particularly when analysing boron-enriched precipitates. The detection system has been recently greatly improved to cope with this phenomenon. Advanced detection signal processing was shown to drastically improve the multihit detection capability of the position sensitive detector [7]. As shown in Fig. 1, and taking into account sampling errors of APT measurements (solid lines), concentration levels given by APT are in good agreement with SIMS measurements (dashed lines) (Fig. 2).

**3 Results** TEM image of samples heat treated at 1000 °C for 1 h reveals the presence of a damaged zone located at a depth comprised between 60 and 140 nm. The atomic map of boron as observed by APT was superimposed (green regions are boron enriched). Clearly, damages revealed by TEM are related to the presence of fairly large boron-enriched regions. This causes the large fluctuations observed in the APT profile shown in Fig. 1. These zones are boron-enriched precipitates.

As shown in Fig. 3, boron-enriched precipitates of few nm in size have already nucleated after implantation

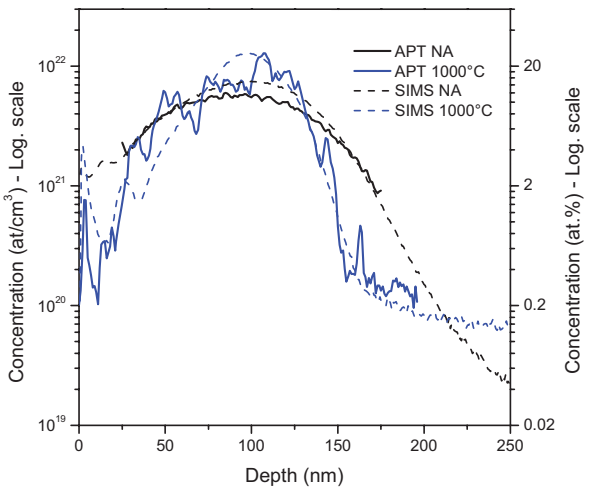


**Figure 1** Comparison of the concentration profiles of boron in the silicon substrate obtained by SIMS (dashed lines) and APT (solid lines) for the NA (black) and 1000 °C (blue) samples. Si wafers were implanted with a very high boron dose ($1 \times 10^{17}$ at. $cm^{-2}$) at 27 keV.

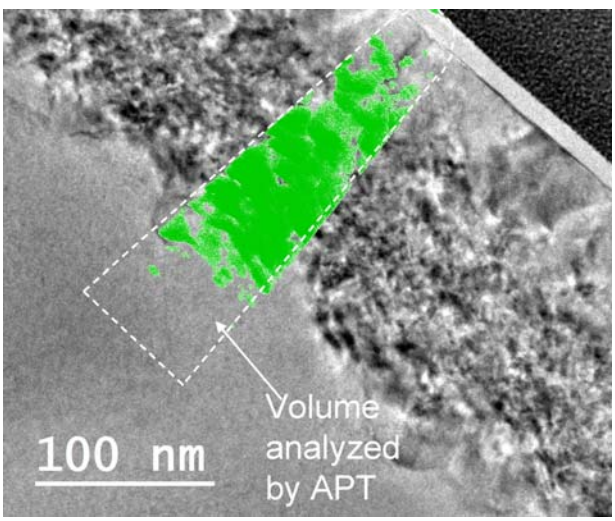


**Figure 2** Superimposition of TEM bright-field image and APT analyses for the 1000 °C sample. Only boron atoms (green dots) are shown for the APT analysis. The limits of the volume of the APT experiment are schematically represented (white dashed lines).

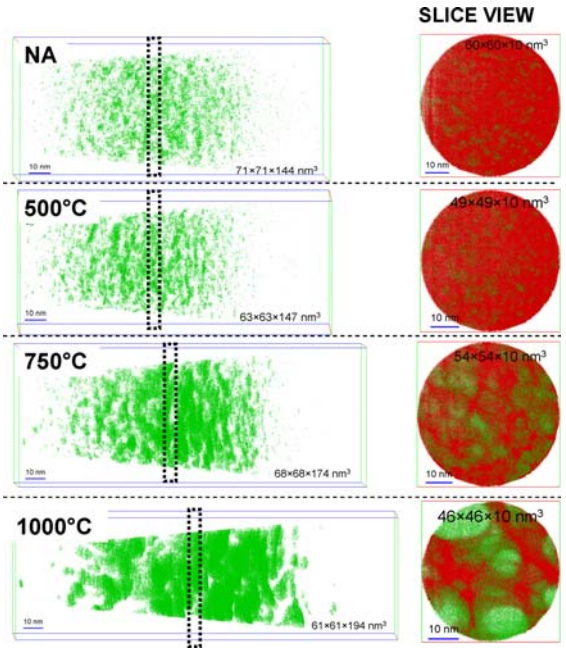


**Figure 3** APT reconstructions for NA, 500, 750 and 1000 °C samples (left). Green dots correspond to boron atoms and red ones to silicon. To enlighten the boron clusters, isosurfaces with a boron concentration > 20 at.% were drawn. A 10-nm thick slice view (right) is associated to each sample to show the boron precipitation. Large precipitates of the known phase $SiB_3$ are observed after 1000 °C annealing.

without any annealing treatment (NA samples). Precipitation during high dose implantation at temperatures where mobility of boron is normally quite low has already been observed and is likely to be caused by dynamic effects. Precipitates appear as isolated particles for this NA state. These boron-enriched clusters have rather large size compared to the so-called BICs [8]. They should not be interpreted as BICs but rather as nuclei of precipitates. BICs are $B_nI_m$ clusters that form as the result of the interaction between $n$ boron atoms with $m$ Si self-interstitial atoms. These BICs, the stability of which may be assessed through *ab initio* and first-principles approaches, are often considered as composed of less than ten atoms. While BICs may exist at concentrations below the solubility limit, boron-enriched nanoprecipitates only nucleate when there is a driving force for precipitation, i.e. boron supersaturation.

To the authors knowledge, no technique is able to image BICs without any ambiguity. Using TEM, Cristiano et al. [9] observed small dislocation loops that were found to be boron decorated and were interpreted as BICs. However, these loops contained a much larger number of atoms than usually considered in BICs. This raises the problem of terminology. Should lattice defects that are enriched in boron be called and identified as BICs? APT is potentially and in principle able to detect these BICs that can be viewed as a short-range order effect. However, these $B_nI_m$ BICs are characterised not only by the clustering of a few boron atoms ($n$) but also by the concomitant presence of $m$ self-interstitial silicon atoms. Unfortunately, APT is unable to discriminate self-interstitial Si atoms and Si atoms in substitution positions. The nature, interstitial or not, of Si atoms observed in boron clusters observed with APT is therefore unknown. As a result, very subtle clustering trends exhibited using APT cannot be proved unambiguously to be BICs or precipitate nuclei. In addition, even in a random solid solution, fortuitous solute clusters exist and may be observed in APT volumes. Only statistical methods such as 1NN (first nearest neighbour) method can face to this issue and provide a nonbiased assessment of clustering [10]. The latter method is based on the distribution of 1NN distances between solute atoms (boron).

As shown in Fig. 3, with increasing temperature, precipitate size increases due to enhanced diffusion at higher temperatures. However, more interestingly, the nanostructure appears more interconnected with precipitates connected to each other. Because of the high volume fraction of precipitates ($f \sim$ overall atomic fraction of boron/atomic fraction of boron in precipitates), one has probably reached the theoretical percolation limits (17% in 3D space for randomly oriented tetrahedra) for annealed samples. For instance the volume fraction is $f \sim 30\%$ at the implantation peak for 750 °C that is much larger than this percolation limit.

**4 Discussion** The phase composition has been plotted as a function of depth for the four heat treatments investigated (Fig. 4). The probed volume was cut in thin slices 10 nm in thickness perpendicular to the depth axis ($z$) so as to get composition profiles as a function of $z$. The atomic fractions of boron in precipitates ($X_\beta$) and in the

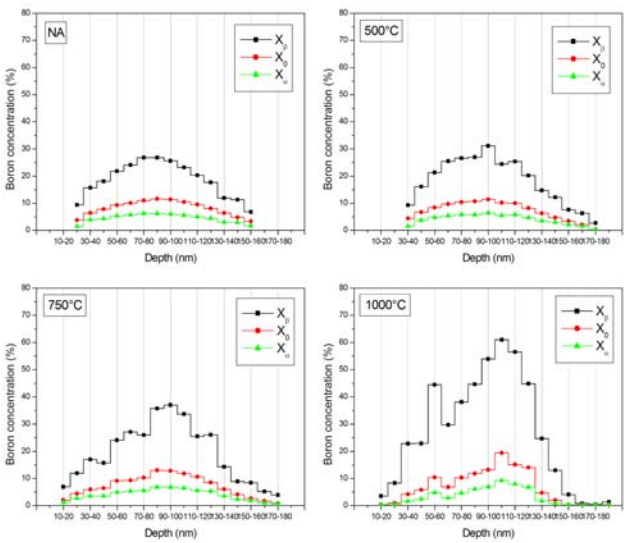


**Figure 4** Depth profiles showing the evolution of phase composition ($X_\alpha$, $X_\beta$) and that of the overall composition ($X_0$) as a function of depth for the four thermal states investigated (not annealed, 500, 750 and 1000 °C).

surrounding parent phase ($X_\alpha$) in these thin slices along the depth scale were derived from APT data using the so-called 1NN method [11]. This latter method was applied in each slice.

$X_\alpha$ and $X_\beta$ profiles are shown to follow that of the overall atomic fraction of boron ($X_0$). Precipitates are observed to contain a smaller amount of boron than that of the $SiB_3$ phase (Fig. 4). This finding may be interpreted within nonclassical nucleation theories that, as a result of the competition between interfacial energy (proportional to the composition gradient at nuclei interface) and nucleation driving force, predict a smaller concentration of solute atoms for increasing nominal composition (i.e. large boron supersaturation) [12]. Profiles and composition measurements demonstrate that with increasing budgets (1000 °C), the composition of precipitates approaches that of the expected $SiB_3$ phase, in good agreement with Cojocaru-Mirédin et al. [13]. Note that the 1NN method may fail to give the right composition of high evaporation field $SiB_3$ precipitates (see Fig. 4 for 1000 °C) because of defocusing effects that give rise to larger 1NN distances than reality [14]. A 75 at.% boron concentration is indeed measured by placing a small box in the clusters observed in Fig. 3 (1000 °C sample).

Note that the boron content (up to 10 at.% at the implantation peak) is much larger than the solubility limit (less than 0.1 at.% in the temperature range considered here). The system is therefore probably above the spinodal line (i.e. instability line for coherent precipitation). A regime of instability is predicted for concentrations between the two inflection points of the free enthalpy G(C) where the second derivative of G(C) is negative. According to this theory, composition fluctuations appear and amplify with ageing time. This decomposition regime that is observed for large supersaturations well inside coherent miscibility gaps, often gives rise to interconnected structures as observed here. FeCr is a typical system where isotropic spinodal decomposition occurs leading to such interconnected structures [15].

Amorphization caused by implantation may modify the location of the spinodal line and consequently the decomposition regime. In addition, boron supersaturation is not constant with depth ($z$) but instead follows the implantation profile ($X_0(z)$, Fig. 4). The phase-separation process in such implants is thus complex as the driving force changes along $z$. The regime (nucleation and growth versus spinodal decomposition) may be different at the implantation peak compared to adjacent regions where the supersaturation is much smaller.

The last item to keep in mind is that the spinodal concept only applies if the early stages of precipitation initiates with the formation of coherent boron-enriched precipitates that have the same diamond structure as silicon (the so-called Guinier–Preston (GP) preprecipitation zones). Such coherent GP zones are metastable and would subsequently transform into the more stable expected $SiB_3$ phase. However, the real structure of boron-enriched zones in the early stages is unknown and the kinetics pathway for the precipitation in SiB system remains an open question. The direct nucleation of nonisostructural $SiB_3$ precipitates cannot be ruled out.

**5 Conclusion** Precipitation of boron in highly supersaturated silicon has been investigated using SIMS, TEM and APT. The results show that precipitates nucleate during implantation before any annealing has been made. Precipitates are observed to form in damaged regions as revealed by TEM. They were found to have a smaller boron content than that of the expected phase $SiB_3$. With increasing thermal budget, the concentration of boron approaches the equilibrium composition (75 at.% of boron). Small boron-enriched precipitated clusters that form in this supersaturated solid solution are considered to be different from the so-called BICs event if self-interstitials may be present in these precipitates. These BICs, composed of a few boron atoms combined with self-interstitial Si atoms, should also be distinguished from boron-enriched lattice defects (e.g. Cottrell atmospheres that are segregation of solute atoms along dislocation lines or dislocation loops) or even precipitates heterogeneously nucleated to lattice defects (e.g. extended defects, dislocations, stacking faults, etc.).

As an extension of the present work, advanced modelling of boron diffusion in heat-treated implants where nucleation and growth of precipitates occur is currently conducted using a new approach compared to what has already been done [16–19].

**Acknowledgements** The authors are grateful the French National Agency for funding through the Project APTITUDE ANR-12-BLANC-00001, to Christiane Dubois from INL for SIMS analyses and to Y. Le Gall from InESS Laboratory for ion implantation.

## References

[1] K. Inoue, F. Yano, A. Nishioda, H. Takamizawa, Y. Nagai, and M. Hasegawa, Ultramicroscopy **109**, 1479–1484 (2009).
[2] J. Bunton, J. Olson, D. Lenz, and T. Kelly, Microscopy Microanal. **13**, 418–427 (2007).
[3] S. Duguay, T. Philippe, F. Cristiano, and D. Blavette, Appl. Phys. Lett. **97**, 242104 (2010).
[4] O. Cojocaru-Mirédin, D. Mangelinck, and D. Blavette, J. Appl. Phys. **106**, 113525 (2009).
[5] B. Gault, F. Vurpillot, A. Vella, M. Gilbert, A. Menand, D. Blavette, and B. Deconihout, Rev. Sci. Instrum. **77**, 043705 (2006).
[6] C. Dubois, G. Prudon, B. Gautier, and J. C. Dupuy, Appl. Surf. Sci. **255**, 1377 (2008).
[7] G. Dacosta, H. Wang, S. Duguay, A. Bostel, D. Blavette, and B. Deconihout, Rev. Sci. Instrum. **83**, 123709 (2012).
[8] P. Pichler, Computational Microelectronics (Springer, Wien, New York, 2004), p. 554.

[9] F. Cristiano, X. Hebras, N. Cherkashin, and A. Claverie, Appl. Phys. Lett. **83**, 5407 (2003).
[10] T. Philippe, F. De Geuser, S. Duguay, W. Lefebvre, O. Cojocaru-Mirédin, G. Da Costa, and D. Blavette, Ultramicroscopy **109**, 1304 (2009).
[11] T. Philippe, O. Cojocaru-Miredin, S. Duguay, and D. Blavette, J. Microscopy **239**, 72–77 (2009).
[12] T. Philippe and D. Blavette, Philos. Mag. **91**, 4606–4620 (2011).
[13] O. Cojocaru-Mirédin, F. Cristiano, P.-F. Fazzini, D. Mangelinck, and D. Blavette, Thin Solid Films **534**, 62–66 (2013).
[14] D. Blavette, F. Vurpillot, P. Pareige, and P. Menand, Ultramicroscopy **89**, 145–153 (2000).
[15] F. Danoix, P. Auger, and D. Blavette, Microsc. Microanal. **10**, 03 (2004).
[16] B. Baccus, E. Vandenbossche, and M. Lannoo, J. Appl. Phys. **77**, 5631 (1995).
[17] M. Uematsu, J. Appl. Phys. **82**, 2228 (1997).
[18] S. Solmi, F. Baruffaldi, and M. Derdour, J. Appl. Phys. **72**, 697 (1992).
[19] H. Bracht, H. H. Silvestri, I. D. Sharp, and E. E. Haller, Phys. Rev. B **75**, 035211 (2007).

 